BELLCOMM, INC.
955 L'ENFANT PLAZA NORTH, S.W.   WASHINGTON, D.C. 20024

B70 09028

SUBJECT: Corrections to the Patched Conic Calculation of Apollo Trajectories - Case 310

DATE: September 11, 1970

FROM: L. P. Gieseler

ABSTRACT

Trajectory dependent corrections to patched conic derived ΔV costs have been determined. These corrections provide a means of obtaining increased accuracy in determining mission opportunities without resorting to precision trajectories. Corrections applicable to lunar orbital insertion, transearth injection, and the DPS abort maneuver are presented.

OCT 1970
RECEIVED
NASA STI FACILITY
INPUT BRANCH

(NASA-CR-113585) CORRECTIONS TO THE PATCHED CONIC CALCULATION OF APOLLO TRAJECTORIES (Bellcomm, Inc.) 13 p

N79-71900

Unclas
00/13 11878

FF No. 602

CR-113585

(PAGES)

(NASA CR OR TMX OR AD NUMBER)

(CODE)

(CATEGORY)

[redacted]

BELLCOMM, INC.
955 L'ENFANT PLAZA NORTH, S.W. WASHINGTON, D.C. 20024

B70 09028

SUBJECT: Corrections to the Patched Conic Calculation of Apollo Trajectories - Case 310

DATE: September 11, 1970

FROM: L. P. Gieseler

MEMORANDUM FOR FILE

I. Introduction

Mission analysis and synthesis for Apollo-type earth-moon trajectories are routinely done using a patched-conic approach. This type of calculation is used because it is much faster than the calculation of precision integrated trajectories. In this memorandum the errors inherent in the patched-conic approximation are determined, and are presented in graphical form. The ΔV costs for a mission designed by using a patched conic analysis can be corrected by adding the appropriate corrections from the graphs.

Corrections are determined by comparing a patched conic and an integrated trajectory, with both subject to the same constraints. These constraints are similar to those used in a mission analysis program, and are discussed more fully in the next section. Two types of errors are determined:

1. Errors caused by neglecting the attraction of the moon outside the moon's sphere of influence (MSI), and the attraction of the earth inside the MSI. (As a result of these assumptions, the geometry of trajectories calculated by the two methods will be somewhat different.)

2. Errors caused by using a velocity impulse (ΔV) rather than a finite powered flight arc. The latter was determined for the lunar orbital insertion (LOI) burn only. However, the results can also be used to correct transearth injection (TEI) ΔV costs.

II. Geometrical Error

A. Description of the Trajectory

A typical non-free return trajectory is shown in Figure 1. The nominal translunar trajectory is represented by curve ABC. At C an LOI burn would normally put the CSM/LM into a circular or elliptical orbit, after which the LM separates and descends to the lunar surface. If the spacecraft propulsion system should fail to ignite, the vehicle coasts for two hours to point D, where a burn using the Descent Propulsion System (DPS) places the vehicle on an orbit which has the proper earth reentry conditions (Curve DEF). Both patched conic and integrated trajectories are shown in the figure.

Three quantities were constrained to have the same value for the two types of calculations. They were:

1. Perigee distance of both translunar and abort portions of the trajectory.

2. Angular location of periselene (θ_p of Figure 1) relative to the earth-moon line.

3. Orientation of the plane of the hyperbola at periselene relative to the lunar orbital plane.

In addition, it was assumed that the periselene altitude of the approach hyperbola equaled the altitude of the lunar parking orbit and that no plane change was required to transfer from one orbit to the other. A velocity impulse (ΔV) was used for the LOI and abort burns in both types of calculations for the determination of the geometrical portion of the error. For LOI, the ΔV was applied at periselene and parallel but opposite to the velocity vector. For the abort case, a two-diminsional optimization was used to establish the abort ΔV direction.

A reference set of trajectories was first generated. These trajectories were located entirely in the moon's orbital plane, and an average earth-moon distance was used. The geocentric energy of the trans-lunar portion of the trajectory was varied, producing trajectories of different flight times and LOI and abort ΔV's. Additional information about this set of trajectories will be found in Appendix I and Table I.

Deviations from the reference set were produced in two ways. The earth-moon distance was changed to a minimum and a maximum value (1.17×10^9 and 1.33×10^9 ft, respectively). Also the dihedral angle (DL_h) between the selenocentric hyperbola and the moon's orbital plane was changed from zero to 15 and 30 degrees. In this way a total of nine sets of trajectories was produced.

Errors were obtained by calculating the patched conic trajectory first. The corresponding integrated trajectory was obtained by using the same position vector at periselene, and the same direction of the periselene velocity vector. The trajectory was then retargeted to the correct constraints for the translunar and abort trajectories by varying the periselene velocity magnitude and the abort ΔV. By this procedure the plane of the lunar parking orbit will have the same orientation relative to the moon for both calculations. Errors were determined by simply differencing the values of the LOI and abort ΔV obtained in the two ways. Because of the symmetry of the translunar and transearth trajectories the errors determined for the LOI maneuver may be applied to the TEI maneuver as well by using appropriate values for the dihedral angle and energy.

B. Results

Figure 2 shows how the error in LOI and TEI ΔV varies as a function of the geocentric energy of the transfer orbit and the dihedral angle of the lunar hyperbola relative to the earth-moon plane. The error varies from about 75 fps at an energy of -10×10^6 ft^2/sec^2 to less than 40 fps at an energy of -6×10^6 ft^2/sec^2. The patched conic calculation gives a ΔV which is less than the integrated calculation.

Figure 3 illustrates the results obtained for the error in abort ΔV. The results have been expressed in terms of percent of the actual abort ΔV required since this value varies from zero for a free return trajectory to a maximum of 2000 fps, the approximate DPS abort capability. For inplane trajectories ($DL_h = 0$) the error is about -5% or -100 fps for a ΔV of 2000 fps. The patched conic calculation gives a required abort ΔV which is greater than the integrated calculation. The error for trajectories having $DL_h = 15°$ is about half of the error at $DL_h = 0$, and the error at $DL_h = 30°$ becomes very small. To compensate for this error, the upper ΔV limit of a patched conic mission analysis program should be set from 0 to 100 fps greater than the desired ΔV limit, depending primarily on the value of DL_h. Additional discussion of both LOI and abort ΔV errors will be found in Appendix I.

III. Powered Flight Error, Lunar Orbital Insertion (LOI)

The error made by using velocity impulse rather than a finite burn for the LOI maneuver is to a large extent decoupled from the geometrical error discussed in Section II, and can be considered separately. Figure 4 illustrates a typical profile for both integrated and impulsive LOI maneuvers. For the integrated trajectory (shown as a solid line in the figure) the initial weight (WGTI) and the specific impulse (I_{sp}) equaled

102,350 lbs and 313.9 sec, respectively. A fixed vehicle attitude in inertial space was used. A measure of the fuel used is the characteristic velocity ΔV_c, defined by the equation

$$\Delta V_c = 32.2 \, I_{sp} \log_e \left(\frac{WGTI}{WGTF} \right)$$

where WGTF is the final weight.

For the impulsive maneuver the vehicle is assumed to travel along the approach hyperbola until periselene is reached. This is shown as a dotted line in Figure 4. At periselene the application of a velocity impulse (ΔV) is assumed. The two trajectories to be compared both start at the ignition point on the approach hyperbola and terminate when the state vector equals that required for the Lunar Parking Orbit (LPO). It can be seen from the figure that the path of the finite burn is very near the path of the approach hyperbola until periselene of the approach hyperbola is reached. At periselene the impulsive ΔV is applied, while the finite burn continues for an additional 9 degrees of central angle. The finite burn also required more maneuver time than the impulsive approximation.

The time of flight from perigee to periselene and the selenocentric energy of four approach hyperbolas are listed in Table II, together with corresponding values of the maneuver time, the central angle, and the value of ΔV. It can be seen that the correction to be added to the impulsive maneuver varies from 190 to 173 sec for maneuver time, from 9.6 to 8.7 degrees for central angle, and from +15.4 to +11.1 fps for ΔV.

As in Section II, the above considerations regarding the LOI burn can be assumed to apply to the TEI burn also. The same corrections can be used for both burns.

IV. Summary and Conclusions

The error made by approximating an Apollo trajectory by a patched conic can be divided into two parts, a geometrical error inherent in the patched conic approximation, and a powered flight error, due to approximating a finite burn by a conic arc and a velocity impulse. For the LOI and TEI burns the patched conic calculation is too low. The error varies from 40 to 75 fps for the geometrical error, and from 15 to 11 fps for the powered flight error, making a total error of from 55 to 86 fps.

The geometrical error alone was calculated for the abort maneuver. For free return trajectories the abort ΔV is zero and there is no error. For non-free return trajectories the abort ΔV rises to 2000 fps (approximately the maximum DPS abort capability) and the patched conic calculation gives values that are too high by a maximum of about 100 fps. Since the conic calculated value is higher than that actually required the limit set for trajectory design should be biased high.

L. P. Gieseler

2013-LPG-slr

L. P. Gieseler

Attachments
Appendix I
Tables I-II
Figures 1-4

APPENDIX I

Insight into the differences between patched conic and integrated trajectories may be obtained by comparison of the values of several common trajectory parameters. These comparisons may be made with the aid of the data given in Table II.

Time of flight from translunar injection to periselene, abort ΔV required, LOI ΔV required and energy data are listed. The conic and integrated trajectories being compared are both targeted to match periselene position and altitude and lunar hyperbola inclination. For the reference set, the hyperbola is in the Earth-Moon plane, the altitude of perilune is 60 nm and the angular position of perilune measured from the Earth-Moon line, θ_p, is varied. Values for θ_p are given in order of increasing value in the table. The patched conic trajectories consistently result in shorter times of flight with the error increasing as total time of flight increases. The conic LOI ΔV costs are also consistently low with the error again increasing as time of flight increases. The errors inherent in the patched conic calculations can be ascribed primarily to the motion of the vehicle in the vicinity of the MSI, where both the earth and the moon have a large influence on the motion. A vehicle in a trajectory with high energy will traverse this region quickly, and accordingly there should be less error.

The error in abort ΔV illustrated in Figure 3 does not show a definite relationship with energy. This can be explained by the fact that the abort portion of the trajectory is influenced not only by the characteristics of the post-abort trajectory, but also by the pre-abort trajectory which controls the state vector at the abort point. As shown in columns 6 and 7 of Table II the energy of the optimum abort trajectory increases while the energy of the pre-abort trajectory decreases.

TABLE I - LOI POWERED FLIGHT

	APPROACH HYPERBOLA		LOI MANEUVER		
	Time hrs.	Energy ft^2/sec^2	Time sec.	Central Angle degrees	ΔV fps
INTEGRATED	68.58	6.041×10^6	401.5	25.9	2989.4
IMPULSIVE			211.4	16.3	2974.0
ERROR			190.1	9.6	15.4
INTEGRATED	78.73	4.340	377.1	24.0	2779.5
IMPULSIVE			197.7	15.0	2766.9
ERROR			179.4	9.0	12.6
INTEGRATED	85.51	3.670	367.1	23.2	2695.5
IMPULSIVE			192.2	14.4	2683.9
ERROR			174.9	8.8	11.6
INTEGRATED	90.46	3.333	362.0	22.8	2652.9
IMPULSIVE			189.4	14.1	2641.8
ERROR			172.6	8.7	11.1

TABLE II - DETAILS OF THE REFERENCE SET OF TRAJECTORIES

	1	2	3	4	5	6	7	8
	Time of Flight, hrs.	Abort ΔV, fps	LOI ΔV, fps	Geocentric Energy*		Selenocentric Energy at MSI*		
				At Perigee	At MSI	Pre-Abort	Post-Abort	θ_P
PATCHED CONIC	68.58	0	2974	-7.652	-7.652	6.041	6.041	0
INTEGRATED	68.66	0	3024	-7.870	-7.531	6.501	6.501	0
DIFFERENCE (I-PC)	.08	0	50	-.218	.121	.460	.460	0
PATCHED CONIC	75.21	821	2825	-8.842	-8.842	4.815	7.566	10°
INTEGRATED	75.46	788	2882	-9.050	-8.802	5.281	8.129	10
DIFFERENCE	.25	-33	57	-.208	.040	.466	.563	0
PATCHED CONIC	78.73	1233	2766	-9.298	-9.298	4.340	8.178	15
INTEGRATED	79.11	1174	2828	-9.497	-9.298	4.814	8.819	15
DIFFERENCE	.38	-59	62	-.199	.000	.474	.641	0
PATCHED CONIC	82.41	1643	2717	-9.677	-9.677	3.941	8.655	20
INTEGRATED	82.98	1569	2783	-9.865	-9.718	4.427	9.389	20
DIFFERENCE	.57	-74	66	-.188	-.041	.486	.734	0
PATCHED CONIC	85.51	1967	2683	-9.934	-9.934	3.670	8.933	24
INTEGRATED	86.27	1883	2753	-10.109	-10.006	4.168	9.749	24
DIFFERENCE	.76	-84	70	-.175	-.072	.498	.816	0
PATCHED CONIC	87.93	2207	2661	-10.102	-10.102	3.491	9.080	27
INTEGRATED	88.88	2116	2733	-10.266	-10.195	4.001	9.962	27
DIFFERENCE	.95	-91	72	-.164	-.093	.510	.882	0
PATCHED CONIC	90.46	2443	2641	-10.250	-10.250	3.333	9.175	30
INTEGRATED	91.62	2346	2717	-10.400	-10.364	3.857	10.125	30
DIFFERENCE	1.16	-97	76	-.150	-.114	.524	.950	0

*Multiply each entry by 10^6. Units are ft^2/sec^2.

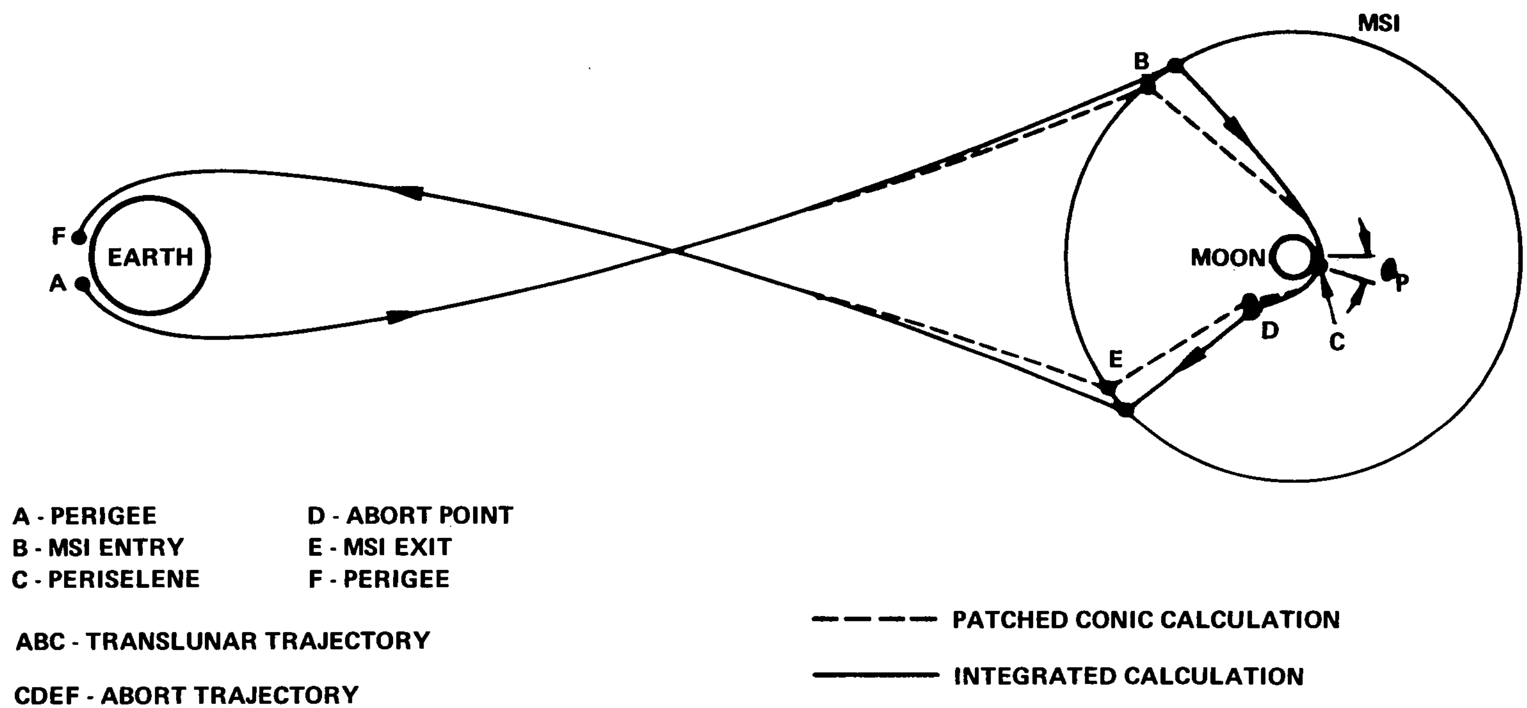

FIGURE 1 - TYPICAL NON-FREE RETURN TRAJECTORY

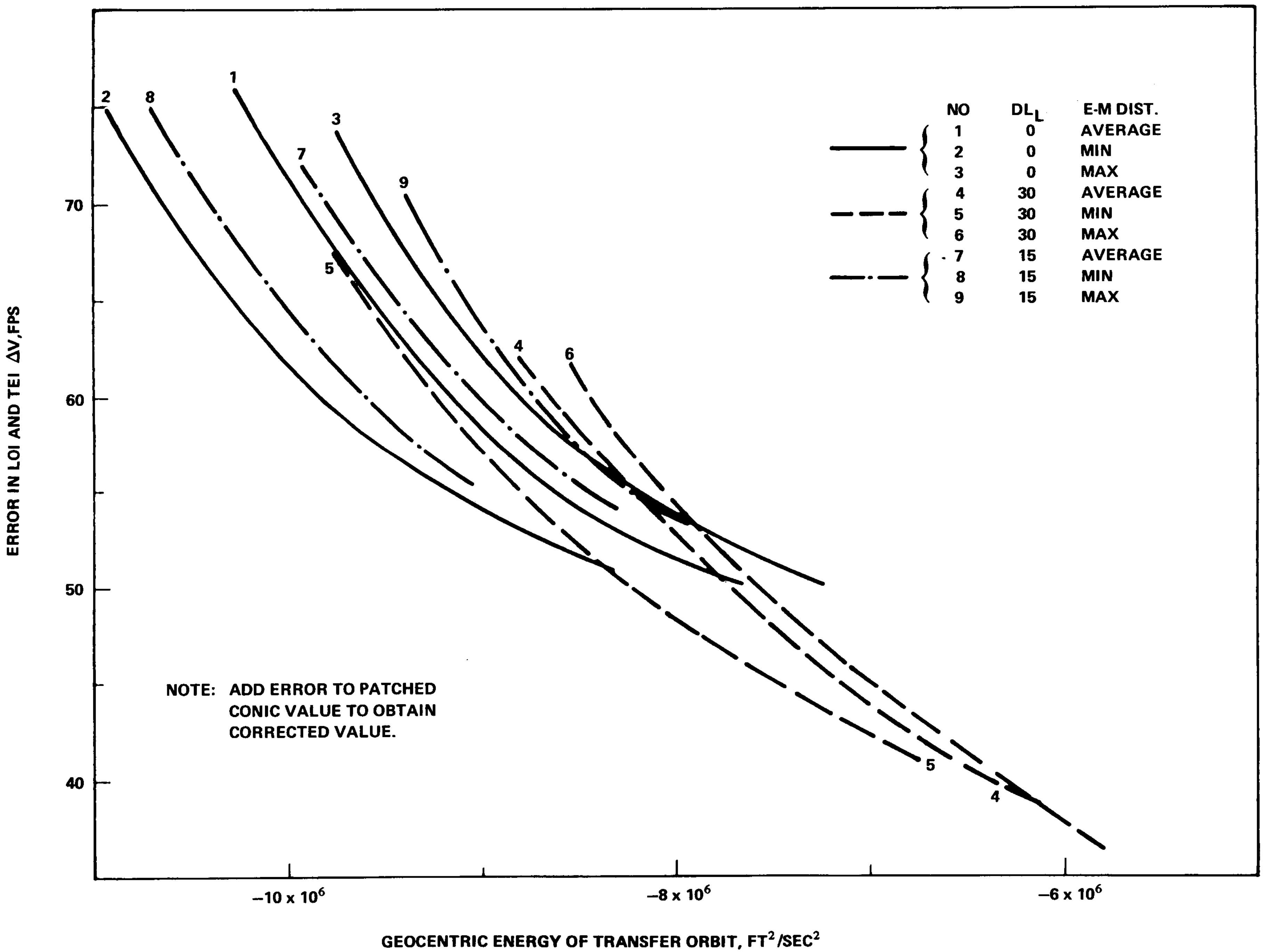

FIGURE 2 - ERROR IN LOI AND TEI ΔV

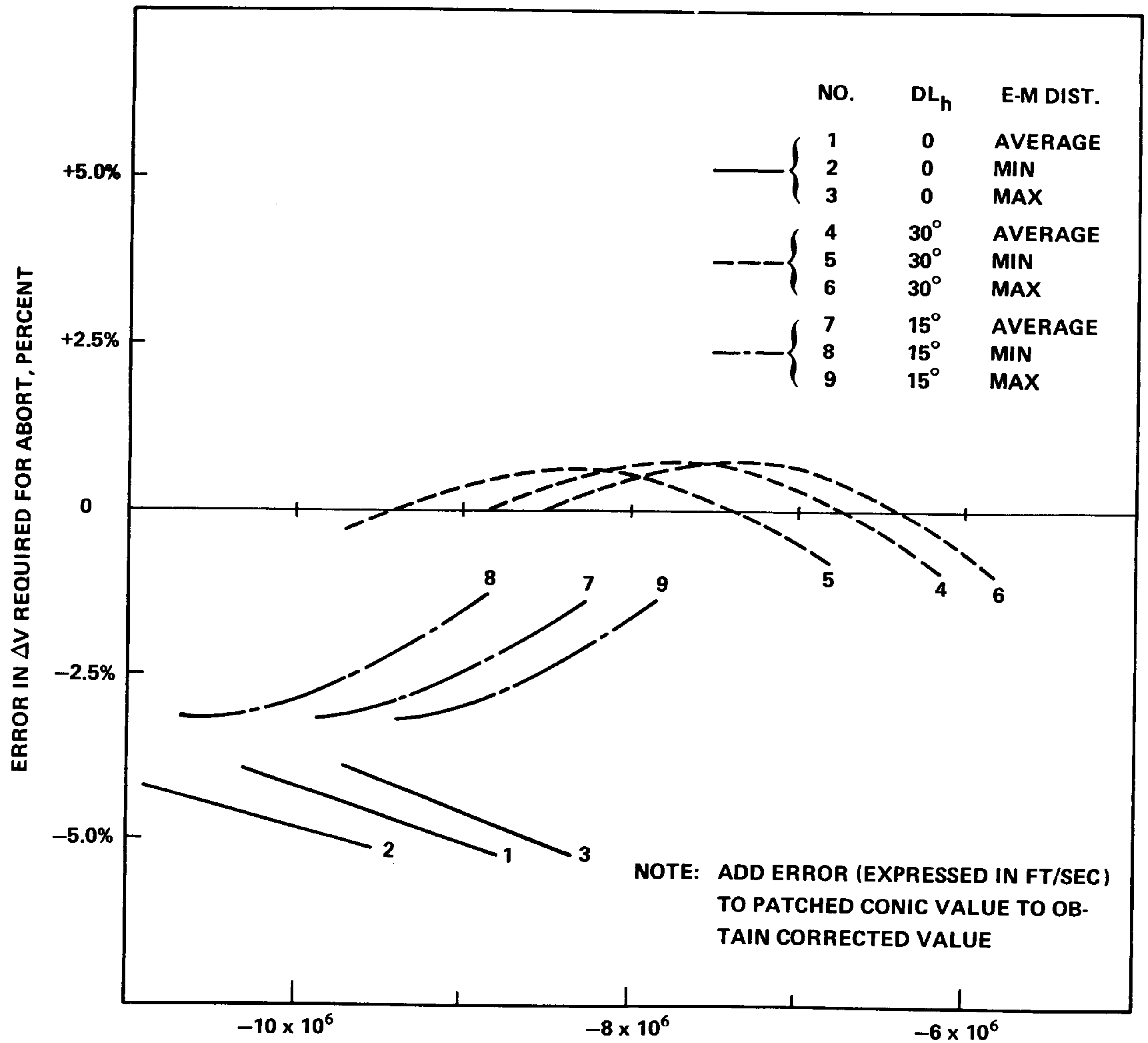

FIGURE 3 - ERROR IN ΔV REQUIRED FOR ABORT

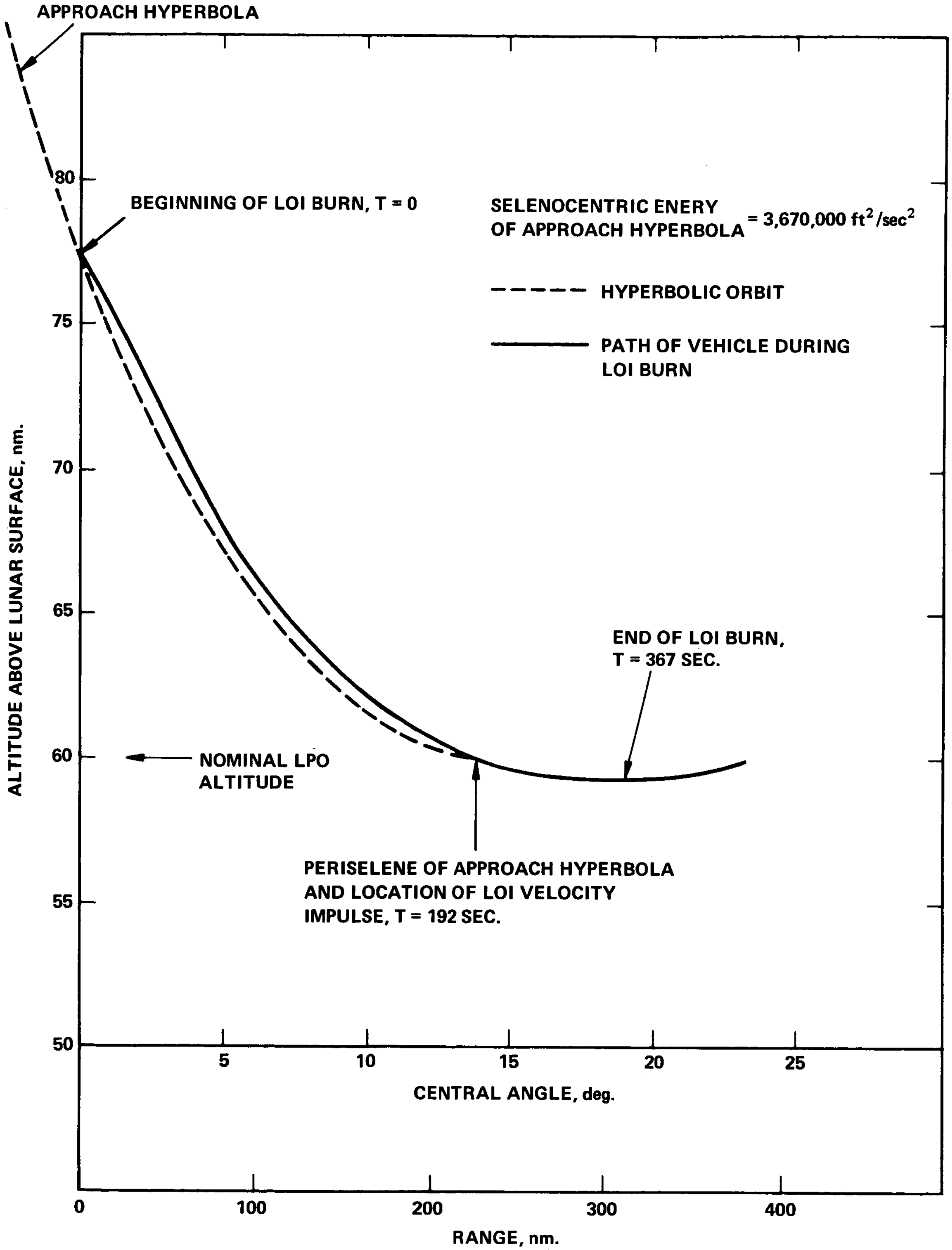

FIGURE 4 - POWERED-FLIGHT AND IMPULSIVE PROFILE FOR LOI BURN

BELLCOMM, INC.

Subject: Corrections to the Patched Conic Calculation of Apollo Trajectories

From: L. P. Gieseler

Distribution List

NASA Headquarters

A. S. Lyman/MR
W. E. Stoney/MAE

Manned Spacecraft Center

R. L. Berry/FM5
A. J. Calio/TA
M. D. Cassetti/FM7
C. Huss/FM
R. H. Kohrs/PD7
G. W. Ricks/FM5

Marshall Space Flight Center

G. Wittenstein/S&E-AERO-MFT

Bellcomm, Inc.

D. R. Anselmo
A. P. Boysen, Jr.
J. O. Cappellari, Jr.
D. A. DeGraaf
F. El-Baz
D. R. Hagner
W. G. Heffron
N. W. Hinners
J. L. Marshall, Jr.
K. E. Martersteck
J. Z. Menard
P. E. Reynolds
J. W. Timko
R. L. Wagner
All Members Department 2013
Central File
Department 1024 File
Library

Abstract Only to

Bellcomm, Inc.

J. P. Downs
I. M. Ross
M. P. Wilson